Heliyon 9 (2023) e20104

Contents lists available at ScienceDirect

Heliyon

journal homepage: www.cell.com/heliyon

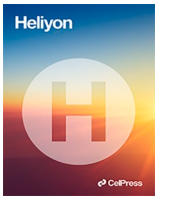

Bushen Huoxue formula for the treatment of diminished ovarian reserve: A combined metabolomics and integrated network pharmacology analysis

Pengfei Zeng [a], Hang Zhou [b], Pei Guo [a], Nana Han [a], Xuan Zhang [a], Zhixing Yin [a], Wanting Xia [a], Jinzhu Huang [c,*], Qian Zeng [a,**]

[a] Department of Gynecology, Hospital of Chengdu University of Traditional Chinese Medicine, Chengdu, China
[b] School of Basic Medicine, Chengdu University of Traditional Chinese Medicine, Chengdu, China
[c] School of Nursing, Chengdu University of Traditional Chinese Medicine, Chengdu, China

ARTICLE INFO

Keywords:
Bushen Huoxue formula
Diminished ovarian reserve
Metabolomics
Network pharmacology

ABSTRACT

Objective: This study aimed to explore the mechanism of the Bushen Huoxue Formula (BHF) in treating diminished ovarian reserve (DOR) through the use of metabolomics and integrated network pharmacology.

Methods: The study involved 24 non-pregnant female Sprague-Dawley rats, divided into four groups of six rats each: control, model, BHF, and DHEA (n = 6 per group). The model group was induced with DOR by administering Tripterygium glycosides orally [50 mg $(kg{\cdot}d)^{-1}$] for 14 days. Subsequently, BHF and Dehydroepiandrosterone (DHEA) treatments were given to the respective groups. Ovarian reserve function was assessed by measuring anti-Müllerian hormone (AMH), estradiol (E_2), and follicle-stimulating hormone (FSH) levels and conducting hematoxylin-eosin staining. In addition, UHPLC-QTOF-MS analysis was performed to identify differential metabolites and pathways in DOR rats treated with BHF. In this study, LC-MS was utilized to identify the active ingredients of BHF, while network pharmacology was employed to investigate the correlations between BHF-related genes and DOR-related genes. An integrated analysis of metabonomics and network pharmacology was conducted to elucidate the mechanisms underlying the efficacy of BHF in treating DOR.

Results: The model group exhibited a poor general condition and a significant decrease in the number of primordial, primary, and secondary follicles ($P < 0.05$) when compared to the control group. However, BHF intervention resulted in an increase in the number of primordial, primary, and secondary follicles ($P < 0.05$), along with elevated levels of AMH and E_2 ($P < 0.05$), and a decrease in FSH levels ($P < 0.05$) in DOR rats. The modeling process identified eleven classes of metabolites, including cholesterol esters (CE), diacylglycerols (DAG), hexosylceramides (HCER), lysophosphatidylcholines (LPC), phosphatidylcholines (PC), phosphatidylethanolamines (PE), sphingomyelins (SM), ceramides (CER), free fatty acids (FFA), triacylglycerols (TAG), and lysophosphatidylethanolamines (LPE). The study found that PC, CE, DAG, and TAG are important metabolites in the treatment of DOR with BHF. LC-MS analysis showed that there were 183 active ingredients in ESI(+) mode and 51 in ESI(−) mode. Network pharmacology analysis identified 285 potential genes associated with BHF treatment for DOR in ESI(+) mode and 177 in ESI(−)

* Corresponding author.
** Corresponding author.
E-mail addresses: huangjinzhu@cdutcm.edu.cn (J. Huang), zqian999d@126.com (Q. Zeng).

https://doi.org/10.1016/j.heliyon.2023.e20104
Received 13 June 2023; Received in revised form 21 August 2023; Accepted 12 September 2023
Available online 13 September 2023

mode. The combined analysis indicated that linoleic acid metabolism is the primary pathway in treating DOR with BHF.

Conclusion: BHF was found to improve ovarian function in rats with DOR induced by Tripterygium glycosides. The study identified key metabolites such as phosphatidylcholine (PC), cholesteryl ester (CE), diacylglycerol (DAG), triacylglycerol (TAG), and the linoleic acid metabolism pathway, which were crucial in improving ovarian function in DOR rats treated with BHF.

1. Introduction

Diminished ovarian reserve (DOR) is a pathological condition that affects women of reproductive age, resulting in reduced fertility due to insufficient ovarian stimulation compared to their counterparts. This decline in fertility can be attributed to a reduction in the quality, quantity, or proliferative capacity of oocytes [1]. Clinical manifestations of DOR include a shortened menstrual cycle and decreased fertility [2].The prevalence of DOR ranges from 10% to 35% and increases gradually [3]. If left untreated, the condition may progress to premature ovarian failure (POF) [4]. Despite extensive research, the pathogenesis of DOR remains unclear and may involve various factors such as genetic predisposition, age-related changes, medically induced injury, immune, environmental, and infectious factors [5].

Current treatment options for DOR include hormone replacement therapy (HRT), antioxidant therapy, dehydroepiandrosterone (DHEA), growth hormone therapy, and assisted reproductive techniques (ART) [6]. However, these therapies are associated with significant side effects, uncertain clinical efficacy, or high costs. The efficacy of HRT in substituting for a functional ovary is controversial, and the well-known risk of venous thromboembolism, stroke, and gynecological cancers associated with HRT further complicates its use [7]. The current evidence does not support the use of DHEA, antioxidant supplementation, or growth hormone therapy to improve ovarian function [8–10]. While assisted ART can help reduce fertility in patients with DOR, the lower quantity and quality of oocytes in these patients often leads to repeated ART cycle failures. Additionally, ART can place a significant financial burden on patients [9,11]. Therefore, alternative treatment options are necessary.

Southeast Asia has utilized Traditional Chinese Medicine (TCM) to address various gynecological endocrine disorders including polycystic ovary syndrome, female infertility, and DOR [12–14]. TCM approaches DOR from a holistic perspective, and studies have shown that traditional Chinese formulas can regulate the hypothalamic-pituitary-ovarian axis (HPOA), prevent ovarian granulosa cell death and oocyte apoptosis, and reduce reproductive toxicity [15–17]. According to TCM theory, DOR is primarily caused by kidney deficiency and blood stasis. The Bushen Huoxue formula (BHF) is a combination of eight Chinese herbal medicines (listed in Table 1) and is based on TCM theory. It is effective in tonifying the kidneys and invigorating the blood. BHF is administered rectally, which allows 50%–70% of the drug to enter circulation directly without the first-pass effect, as opposed to traditional oral administration. Rectal administration also prevents the destruction of the drug by gastrointestinal digestive enzymes, improving its bioavailability and avoiding degradation or instability due to the relatively constant environment in the rectum [18,19]. Previous studies have also shown that BHF improves endometrial interstitial cell chemotaxis and promotes angiogenesis [20]. However, due to the multi-target and multi-substance nature of BHF, investigating its potential mechanism in treating DOR is challenging. Metabonomics studies the human body as a dynamic complete system, which is similar to the principle of wholeness and dynamics of TCM [21]. Network pharmacology systematically observes the effects of drugs on diseases based on disease-gene-drug interaction networks and reveals the mechanism of action of drugs in treating diseases [22]. The combination of metabolomics and network pharmacology is useful for unraveling the multi-component and multi-target mechanisms of BHF.

This study utilizes UHPLC-QTOF-MS to identify differential metabolites to investigate the efficacy of BHF in treating DOR. The study also employs LC-MS to identify the active ingredients of BHF and network pharmacology to elucidate correlations between BHF-related genes and DOR-related genes. Ultimately, the integrated analysis of metabonomics and network pharmacology provides insights into the mechanisms underlying the efficacy of BHF in treating DOR.

Table 1
The ingredients in BHF.

English Name (Chinese Name)	Latin Name	Place of origin	Crude Herb (g)
Cuscutae Semen (Tusizi)	*Cuscuta chinensis Lam.*	Sichuan	15g
Rubi Fructus (Fupenzi)	*Rubus chingii Hu*	Zhejiang	10g
Fructus Lycii (Gouqi)	*Lycium barbarum* L.	Ningxia	10g
Salvia miltiorrhiza (Danshen)	*Salvia miltiorrhiza Bge.*	Sichuan	10g
RadixDipsaci (Xuduan)	*Dipsaci Radix*	Sichuan	20g
Maybush (Shanzha)	*Crataegus pinnatifida Bge.Var.major N.E.Br.*	Shanxi	15g
Chinese Yam (Shanyao)	*Dioscorea opposite Thunb.*	Henan	15g
Retinervus Luffae Fructus (Sigualuo)	*Luffa cylindrica (L.) Roem.*	Sichuan	15g

2. Materials and methods

2.1. Experimental animals

In this study, we selected a total of 30 six-week-old female Sprague-Dawley (SD) rats with specific pathogen-free (SPF) status and a body weight of (200 ± 20) g from Chengdu Dossy Experimental Animal Co., LTD (license number: SCXK(CHUAN) 2020-030).

The rats were housed in the animal laboratory of Hi-Tech Zone Chengdu Tianhe Biology and Medical Industry Incubation Park under a 12:12-h light-dark cycle, with standard feed and drinking water. The room temperature was maintained at 20–24 °C, and the relative humidity was set at 52%–62%, with three rats per cage. The animal protocol for the study was approved by the ethics committee of the Hospital of Chengdu University of TCM (reference number: 2019DL-006).

2.2. Preparation of Chinese herbal medicine

BHF is a granule mix of Chinese herbal medicine obtained from the pharmacy of the Hospital of Chengdu University of TCM. Table 1 presents information about the ingredients and types of Chinese herbal medicine used in BHF.

2.3. Experimental protocol

Following a seven-day acclimatization period, a cohort of 24 female rats with a regular estrous cycle were selected based on vaginal smears. The rats were then randomly assigned to one of four groups, including the control group (A, n = 6), the model group (B, n = 6), the BHF group (C, n = 6), and the DHEA group (D, n = 6). The weight (kg) of each rat was recorded.

To study the effect of Tripterygium glycosides on the DOR model, the model group, BHF group, and DHEA group were given an oral dose of 50 mg·(kg·d)$^{-1}$ for 14 days, from day 8–21. The control group, on the other hand, received an equal volume of 0.9% sodium chloride solution orally for 14 days, from day 8–21. The Tripterygium glycosides were obtained from Shanghai Fudan Fuhua Pharmaceutical Co., Ltd., Z31020415, Shanghai, China.

The therapeutic intervention was administered once daily at 9:00 a.m. for 10 consecutive days, starting from day 22–31. The control and model groups were given 1 mL·(kg·d)$^{-1}$ of 0.9% sodium chloride solution enema and orally administered with 1 mL·(kg·d)$^{-1}$ of 0.9% sodium chloride solution. The BHF group was given 1 mL·(kg·d)$^{-1}$ of BHF suspension (approximately 0.2205 g·kg^{-1} of Chinese herbal medicine granule mix) enema (refer to Fig. 1) and orally administered with 1 mL·(kg·d)$^{-1}$ of 0.9% sodium chloride solution. The DHEA group was given 1 mL·(kg·d)$^{-1}$ of 0.9% sodium chloride solution enema and orally administered with 1 mL·(kg·d)$^{-1}$ of DHEA suspension (approximately 4.815 mg·kg^{-1} of DHEA, GNC Holdings Inc., CODE543822, Hongkong, China).

2.4. Determination of estrus cycle

In this study, a sterile fine cotton swab was used to collect epithelial cells from the vagina of female rats. The swab was soaked in a 0.9% sodium chloride solution and gently inserted approximately 0.5 cm into the vagina, rotated clockwise and counterclockwise on a slide to ensure an even coating of the secretion. The morphology of the collected cells was analyzed using an Olympus CX21 light microscope. The estrous cycle of adult female rats typically consists of four phases: proestrus, estrus, metestrus, and diestrus, which last for 4–5 days. An altered estrous cycle is defined as a cycle that is prolonged (≥6 days), incomplete, or if the rat remains in a single phase for more than 3 days. The specific criteria for determining the estrous cycle are presented in Table 2.

2.5. Histomorphological examination of the ovary

The left ovarian tissues were fixed in 4% paraformaldehyde for 48 h. They were then dehydrated using a gradient of alcohol and embedded in paraffin. The resulting specimen was cut into 3 μm sections and stained with HE (Sciarray Biologicals Co., Ltd., China). The cell morphology of follicles at all levels and atretic follicles in the ovarian tissue were examined using an Olympus CX21 light microscope (Japan).

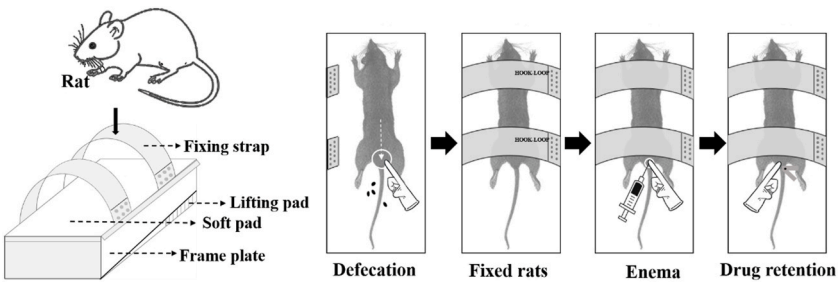

Fig. 1. Schematic diagram of the enema administration operation procedure.

Table 2
Criteria for determination of estrus cycle in rats.

Estrus cycle	Light mirror image
proestrus	Cells almost nucleated epithelial cells, occasionally a few keratinized cells
estrus	The cells are all non-nucleated keratinized cells, accumulating in a deciduous pattern, with a few nucleated epithelial cells interspersed
metestrus	Leukocytes, keratinocytes and nucleated epithelial cells all three, with a preponderance of nucleated epithelial cells
diestrus	Large number of leucocytes and small amount of epithelial cells and mucus

2.6. Enzyme-linked immunosorbent assay (ELISA)

The collected blood specimens were centrifuged at a speed of 2000 r·min^{-1} for a duration of 10 min to obtain serum. The serum was then stored in a refrigerator at a temperature of 4 °C. To measure the expression of serum anti-müllerian hormone (AMH), follicle-stimulating hormone (FSH), and estradiol (E_2), ELISA was used following the instructions provided by Elabscience Biotechnology Co., Ltd, China.

2.7. Metabolomics analysis

The UHPLC separation was carried out using a SCIEX ExionLC series UHPLC System. The mobile phase A was made up of 40% water, 60% acetonitrile, and 10 mmol/L ammonium formate, while mobile phase B consisted of 10% acetonitrile and 90% isopropanol, and 10 mmol/L ammonium formate. The column temperature was maintained at 40 °C, and the auto-sampler temperature was set to 6 °C with an injection volume of 1 μL.

Details of the liquid chromatography flow conditions are provided in Table 3. The assay development was performed using an AB Sciex QTrap 6500+ mass spectrometer with the following ion source parameters: IonSpray Voltage at +5500/-4500 V, Curtain Gas at 40 psi, Temperature at 350 °C, Ion Source Gas 1 at 50 psi, Ion Source Gas 2 at 50 psi, and DP at ±80V.

To quantify the target compounds, we used the Skyline 20.1 Software. We calculated the absolute content of individual lipids by using the peak area and the actual concentration of the identical lipid class internal standard (IS). After that, we obtained the absolute content by averaging the diverse internal standards of the identical lipid class.

To analyze the data of detected metabolites, we employed principal component analysis (PCA). We obtained qualitative and quantitative results using Student's t-test and orthogonal projections to latent structures-discriminant analysis (OPLS-DA). We selected differential metabolites with VIP >1 and $P < 0.05$, and analyzed these significant metabolites using MetaboAnalyst 5.0 (http://www.metaboanalyst.ca/) [23] for pathway analysis. We considered pathways with $P < 0.05$ as potential pathways [24].

2.8. Establishment of an ingredient-gene-DOR network

In this experiment, three samples of BHF were added to each of the 2.0 mL centrifuge tubes. Then, 800 μL of 80% methanol was added and the tubes were vortexed thoroughly to ensure homogeneous mixing. After that, the tubes were left to stand at −20 °C for 60 min before being centrifuged at 12,000 r·pm^{-1} for 15 min. Supernatant (200 μL) was collected and mixed with 5 μL of IS (0.14 mg/mL dichloro phenylalanine) before being stored at 4 °C prior to LC-MS analysis.

To separate the target active ingredients, a UHPLC system and a Thermo Q Exactive mass spectrometer were used. Separation was achieved on an ACQUITY UPLC HSS T3 column (100 × 2.1 mm, 1.8 μm) with linear gradient elution using solvents A (0.1% formic acid in water) and B (acetonitrile). The column temperature was maintained at 4 °C, and the injection volume was 5 μL (refer to Table 4).

The mass spectrometry detection parameters were set as follows: spray voltage was set at 3000 V for ESI+ and 3200 V for ESI−, heater temperature was set at 300 °C, capillary temperature was set at 350 °C, sheath gas flow rate was set at 45 arb, aux gas flow rate was set at 15 arb, sweep gas flow rate was set at 1 arb, and S-Lens RF level was set at 30% for ESI+ and 60% for ESI−.

The active ingredients of BHF were obtained from the PubChem database (https://pubchem.ncbi.nlm.nih.gov/). To predict the gene information for these ingredients, the SwissTargetPrediction database (http://www.swisstargetprediction.ch/) was utilized with a score >0. A search was conducted using the term 'diminished ovarian reserve' in GeneCards (https://www.genecards.org/), and genes with a score >3.75 were selected as candidate genes. The Venny tool (https://bioinfogp.cnb.csic.es/tools/venny/) was used to select the intersection genes of BHF-related and DOR-related genes as key genes. The protein-protein interaction (PPI) network was

Table 3
Flow phase conditions for UHPLC-QTOF-MS.

Time/min	Flow/(μL·min^{-1})	A%	B%
0	300	80	20
1	300	80	20
4	300	40	60
15	300	2	98
16	300	2	98
16.01	300	80	20
18	300	80	20

Table 4
Flow phase conditions for LC-MS.

Time/min	Flow/(μL·min^{-1})	A%	B%
0	300	95	2
1	300	95	2
12	300	5	50
13.5	300	55	50
13.6	300	95	22
1	300	95	2

created through the use of STRING 11.5 (https://STRING-db.org/). The significant genes were then inputted into Metascape (https://metascape.org/gp/index) [25] and Cytoscape 3.9.1 to generate a compound-genes-pathway network, which illustrates the interaction among BHF's active ingredients, genes, and pathways.

2.9. Integrated analysis of metabolomics and network pharmacology

In the ovarian metabonomics analysis, significant pathways ($P < 0.05$) were identified and compared with pathways obtained from the network pharmacology analysis to find any overlaps. Using a reverse search approach, potential active ingredients and genes related to BHF were identified from the overlapping pathways. Finally, the potential active ingredients, genes, and metabolic pathways of BHF that influence DOR were determined.

2.10. Statistical analysis

IBM SPSS Statistics 25.0 software was used for statistical analysis. One-way analysis of variance (ANOVA) was employed for data that met the assumptions of normal distribution and homoscedasticity, while Kruskal-Wallis was used for data that did not meet these assumptions. Statistical significance was set at $P < 0.05$. GraphPad Prism 9.0 (GraphPad Software Inc., San Diego, USA) was used for data visualization.

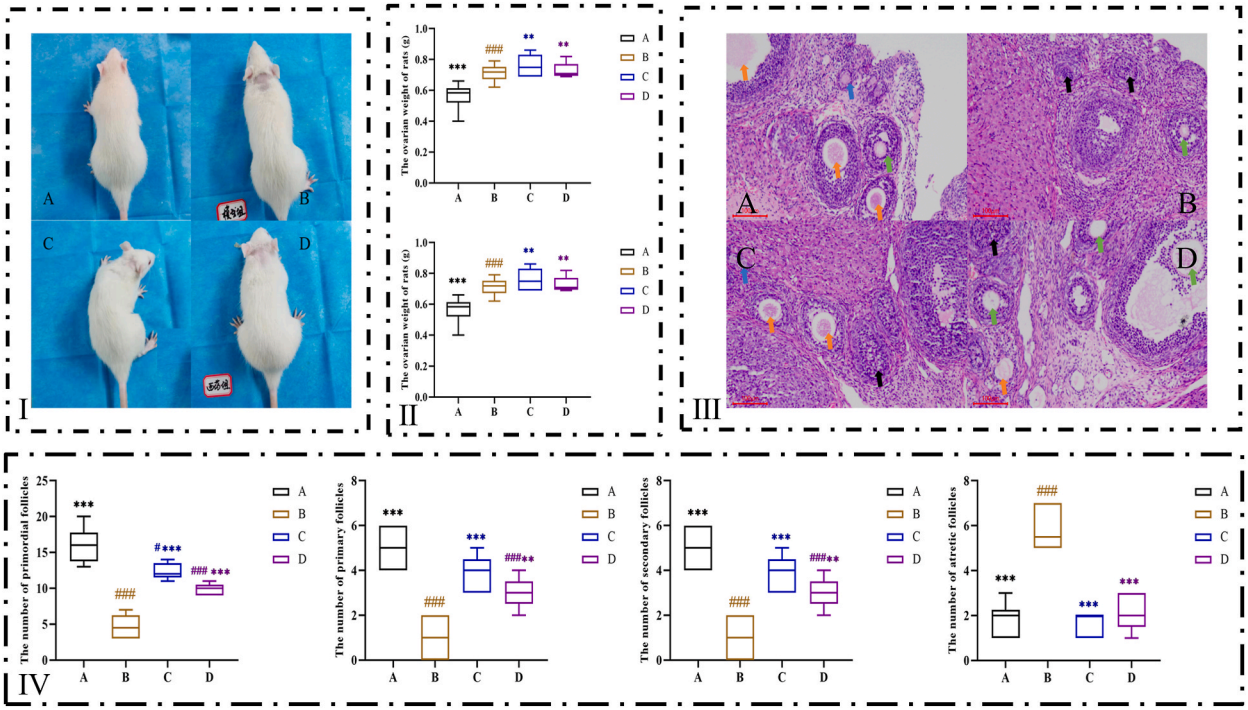

Fig. 2. General condition of rats and histomorphological examination of the ovary. A - the control group, B - the model group, C - the BHF group, D - the DHEA group. I: Comparison of the appearance of the rats in each group. II: Comparison of ovarian weight and ovarian organ index of rats in each group. $^{**}P < 0.01$, $^{***}P < 0.001$ vs the model group; $^{\#\#\#}P < 0.001$ vs the control group. III: Comparison of ovarian pathological sections of rats in each group (HE, × 100). The blue arrows represent the primordial follicles, green arrows represent primary follicles, orange arrows represent secondary follicles and black arrows represent atretic follicles. IV: Follicle counts of each group. **P < 0.01, ***P < 0.001 vs the model group; ###P < 0.001 vs the control group.

PCA was used to analyze the detected metabolites. Student's t-test and OPLS-DA were employed for qualitative and quantitative analysis of the results. Differential metabolites were identified using Student's t-test, OPLS-DA, $VIP > 1$, and $P < 0.05$.

3. Results

3.1. General condition of rats and histomorphological examination of the ovary

During the modeling process, one rat in the DHEA group died on day 17, while another rat in the model group died on day 19. The rats exhibited respiratory distress after gavage, which could have been attributed to the drug injection into the lungs, leading to their immediate decapitation or euthanasia. In contrast, rats in the control group displayed normal behavior, response, diet, hair color, blood supply to the ears, paw nails, tail, defecation, and vigor. The rats in the model group exhibited slower movement, huddling, inactivity, unresponsiveness, dry, sparse, and lusterless hair, especially on the head and neck, dry paw nails, thin and soft stools, and pale ears and tongue. However, the rats in both the BHF and DHEA groups showed normal locomotor response and diet, with pale white ears, tongues, tails, and soft stools as depicted in Fig. 2, panel I.

After 14 days of intervention, the ovarian weights of rats in the model group were significantly lower than those in the control group ($P < 0.001$). However, the ovarian weights of rats in both the BHF and DHEA groups were significantly greater than those in the model group ($P < 0.01$). The ovarian index also showed a similar trend, with a significant reduction in the model group compared to the control group ($P < 0.001$) and improvement in both BHF and DHEA treatment groups ($P < 0.01$ for the BHF group and $P < 0.001$ for the DHEA group). Notably, there was no significant difference in ovarian weight or ovarian index between the BHF and DHEA groups, as shown in Fig. 2, panel II.

The ovarian tissues of rats in the model group showed reduced in normal follicles, disruption in follicular structure, wrinkled follicular zona pellucida, an increase in atretic follicles, and an increase in granulosa cells, as shown in Fig. 2, panels III and IV. The number of primordial, primary, and secondary follicles at all levels was lower than that of the control group ($P < 0.05$). Following the therapeutic intervention, the number of primordial, primary, and secondary follicles in the BHF group was closer to normal, with some observable atretic follicles. The follicle counts at all levels, including primordial and primary follicles, were significantly reduced compared to the control group ($P < 0.05$). Compared to the model group, there was a significant increase in the number of primordial, primary, and secondary follicles. In the DHEA group, the number of follicles at all levels was closer to normal, with a slight increase in the number of observable atretic follicles. The BHF and DHEA groups had slightly lower numbers of follicles at all levels and decreased numbers of primordial, primary, and secondary follicles compared to the control group ($P < 0.05$). However, these values still showed a significant increase compared to the model group ($P < 0.05$).

3.2. BHF improves the reproductive hormone level in DOR rats

The study aimed to investigate reproductive hormone levels (AMH, E_2, and FSH) secreted by rats in different groups. Fig. 3 shows that AMH and E_2 levels were significantly lower in rats from the model group compared to the control group ($P < 0.001$ and $P < 0.05$ respectively), while FSH levels were significantly higher in the model group ($P < 0.001$). However, rats treated with BHF and DHEA had significantly higher AMH and E_2 levels ($P < 0.05$) and lower FSH levels ($P < 0.05$) compared to the model group. These findings suggest that BHF and DHEA can effectively increase AMH and E_2 levels and decrease FSH levels in rats with DOR.

3.3. Metabolomics analysis identified the differential metabolism of BHF in DOR rat

In order to investigate the metabolic roles of BHF in DOR, this study conducted a comprehensive analysis of differential metabolites in ovarian samples from DOR rats. The results of the PCA analysis presented in Fig. 4, panel I, showed that the majority of the samples were concentrated within the 95% confidence interval of the scatter plot. Additionally, there was no significant separation observed in the overlap of the quality control (QC) samples, indicating that the experimental results were reproducible. To ensure the reliability of the OPLS-DA model, multiple permutations (n = 200) were performed by randomly altering the order of the categorical variable *Y*. The results displayed in Fig. 4, panel II, indicate that the distance between the Q^2 regression line and the *Y*-axis was less than zero,

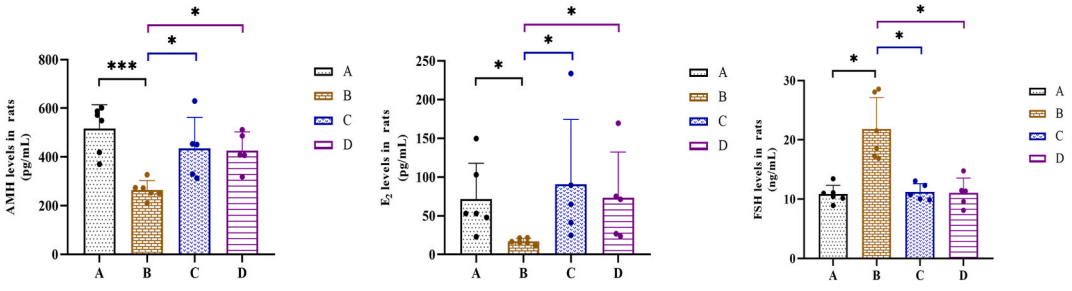

Fig. 3. Comparison of serum AMH, FSH and E_2 in each group. A - the control group, B - the model group, C - the BHF group, D - the DHEA group. *$P < 0.05$, **$P < 0.01$, ***$P < 0.001$ vs the model group.

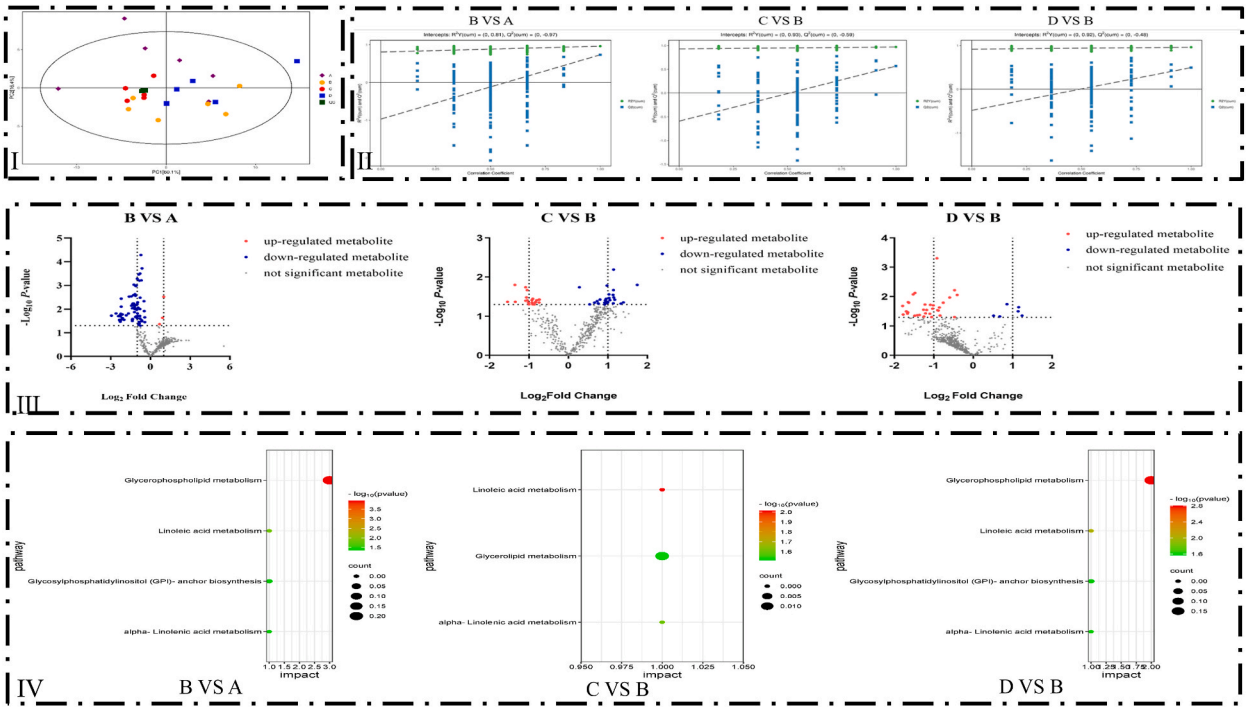

Fig. 4. Metabolomics analysis identified the differential metabolism of BHF in DOR rat. A - the control group, B - the model group, C - the BHF group, D - the DHEA group. I: PCA score plot of metabolites of rat ovarian tissue. II: Replacement map of the OPLS-DA model of rat ovarian tissue metabolite. III: Volcano map of differential metabolites of ovarian tissue in rats. IV: The enrichment analysis of differential metabolites.

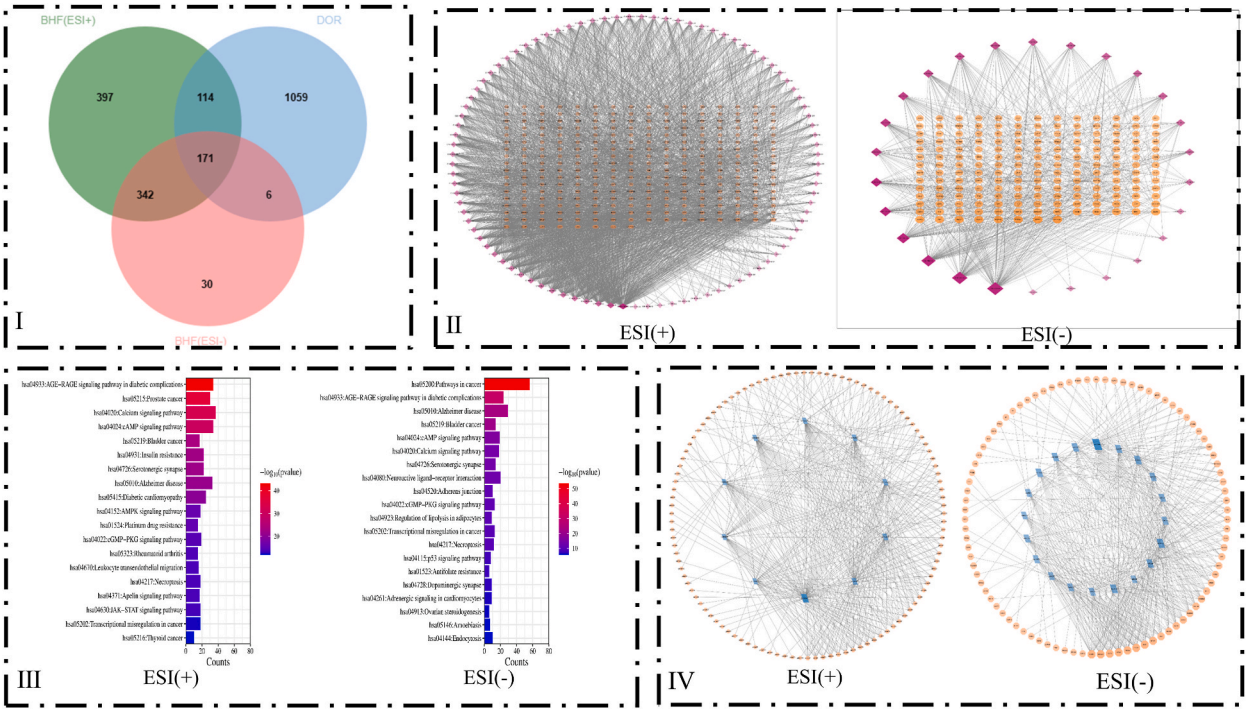

Fig. 5. Network pharmacology predicted the potential genes of BHF on DOR. I: The Venn analysis showed the crosstalk of DOR in BHF. II: PPI network of BHF's compound targets against DOR. The nodes with orange hexagon represent the genes, the nodes with rosy diamond represent the BHF'S active ingredients. III: Gene-pathway signal network. The nodes with blue parallelogram represent the pathway, the nodes with orange hexagon represent the genes. IV: The KEGG pathways enrichment analysis.

indicating that the model was dependable and not susceptible to overfitting [26].

The objective of this study was to investigate the metabolic roles of BHF in DOR by analyzing differential metabolites in ovary samples from rats. *VIP* > 1 and $P < 0.05$ were used as screening criteria to identify differential metabolites. The results were presented in the form of volcano plots (refer to Fig. 4, panel III). In the comparison between the model group and the control group, a total of 78 differential metabolites were obtained. Out of these, 75 were down-regulated, including Cholesterol Esters (CE), Diacylglycerols (DAG), Hexosylceramides (HCER), Lysophosphatidylcholines (LPC), phosphatidylcholines (PC), Phosphatidylethanolamines (PE), Sphingomyelins (SM), and Ceramides (CER). Additionally, three metabolites showed an upward trend, all of which were Triacylglycerols (TAG) (Table S1). In the study, a comparison was made between the BHF group and the model group, revealing 49 differential metabolites. Of these, 28 metabolites were down-regulated, including free fatty acids (FFA) and TAG, while 21 metabolites were up-regulated, including PC, DAG, and CE (Table S2). Similarly, a comparison between the DHEA group and the model group showed 39 identified metabolites. Of these, 6 metabolites showed a down-regulation trend, including lysophosphatidylethanolamines (LPE), FFA, and TAG, while 33 metabolites showed an up-regulation trend, including SM, PE, PC, LPE, hexCer, DAG, Cer, and CE (Table S3). The study found that PC, CE, DAG, and TAG were identified as shared differential metabolites between the model group vs control group and BHF group vs model group comparisons. This suggests that these metabolites are crucial in improving ovarian function in rats treated with BHF.

The MetaboAnalyst platform was used to perform KEGG enrichment analysis of differential metabolites to investigate the potential metabolic pathways involved in the effect of BHF on DOR rats. The analysis results revealed that linoleic acid metabolism, alpha-Linolenic acid metabolism, and glycerolipid metabolism were potential metabolic pathways, as shown in Fig. 4, panel IV. Thus, it can be concluded that BHF can enhance ovarian function in DOR rats by regulating specific metabolites and metabolic pathways. These findings provide new insights into the potential mechanisms underlying the therapeutic effect of BHF on DOR.

3.4. Network pharmacology predicted the potential genes of BHF on DOR

Using LC-MS analysis, we were able to identify 183 active ingredients in ESI(+) mode and 51 active ingredients in ESI(−) mode. The chemical structures of these active ingredients were retrieved from the PubChem database, and we were able to extract 1024 genes in ESI(+) mode and 549 genes in ESI(−) mode from the SwissTargetPrediction database. Additionally, we extracted 1350 genes related to DOR from the Genecard database. By analyzing this data, we were able to identify 285 potential genes in ESI(+) mode and 177 potential genes in ESI(−) mode that are related to BHF treatment of DOR (refer to Fig. 5, panel I). To display the complex relationship between BHF active ingredients and potential DOR genes, we constructed an active component-gene network (refer to Fig. 5, panel II).

Based on the degree of connectivity, the top ten active ingredients in ESI(+) mode were oroxylin A, apigenin, resveratrol, isoxanthohumol, kaempferol, sinapic acid, 4-methyl-6,7-dihydroxy coumarin, isorhamnetin, loureirin B, and norisoboldine, while the top ten active ingredients in ESI(−) mode were glabridin, alpinetin, xanthohumol, pectolinarigenin, phenethyl caffeate, herbacetin, 8-Prenylnaringenin, demethoxycurcumin, licochalcone C, and piceatannol.

To identify key genes of BHF in treating DOR, a protein-protein interaction (PPI) network was constructed. The average node degree was found to be 7.31 in ESI(+) mode and 6.29 in ESI(−) mode. The top ten nodes with a degree greater than the average were selected, revealing CYP19A1, ESR2, CA2, CA9, ESR1, EGFR, ALOX5, ACHE, AKR1B1, and MAOA as key targets in ESI(+) mode, and CYP19A1, PTPN1, AKR1B1, MAOB, PTGS1, ADORA1, CA2, ALOX5, EGFR, and ESR1 as key targets in ESI(−) mode.

In order to explore the mechanisms of BHF treatment of DOR, we conducted KEGG enrichment analysis on the identified genes. Our findings, as shown in Figure panel 5 III, indicate that BHF treatment of DOR may be closely related to various intervened pathways such as ovarian steroidogenesis, cAMP signaling pathway, serotonergic synapse, cGMP-PKG signaling pathway, and calcium signaling pathway. Additionally, we extracted the signaling pathways related to DOR from the KEGG database and utilized Cytoscape software to generate a target-pathway network, as illustrated in Fig. 5, panel IV.

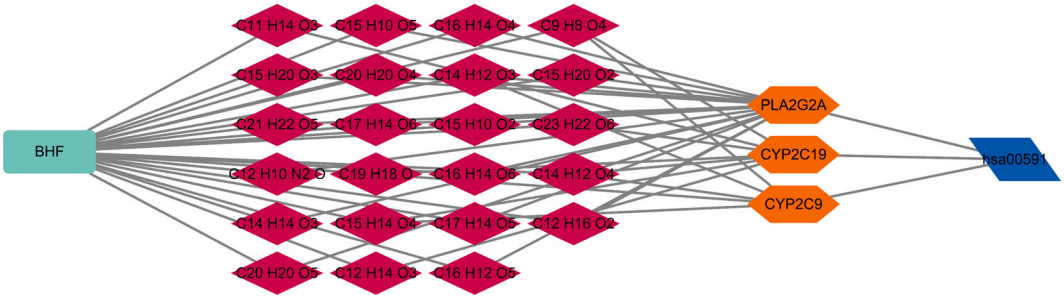

Fig. 6. Combined network pharmacology and metabolomics to analyze the formula-active ingredients-gene-pathway network of BHF in DOR. The nodes with indigo blue round rectangle represent BHF, the nodes with rosy diamond represent the BHF'S active ingredients, the nodes with orange hexagon represent the gene, and the nodes with blue parallelogram represent the pathway.

3.5. Integrated analysis of metabolomics and network pharmacology

In order to gain a comprehensive understanding of how BHF treats DOR, we utilized metabolomics and network pharmacology to establish an interaction network. Our analysis demonstrated that BHF's therapeutic effects on DOR are achieved through the modulation of 27 active ingredients, 3 genes, 1 metabolite, and 1 metabolic pathway (refer to Fig. 6 for visualization).

4. Discussion

This study explores the potential of TCM in treating DOR, a complex gynecological endocrine disorder that is often associated with female infertility and POF [4,27]. While modern medical treatments have limitations, TCM offers unique advantages and a rich history of experience in treating similar disorders. The study uses UHPLC-QTOF-MS and LC-MS to investigate the potential of BHF, a TCM remedy, in mitigating DOR induced by Tripterygium glycosides in rats. Additionally, network pharmacology is used to predict the potential genes of BHF on DOR. By combining metabolomics and network pharmacology, the study aims to decipher the mechanisms of BHF in treating DOR.

The study found that administering Tripterygium glycosides to model rats for 14 days resulted in a significant decrease in their body weight. Further analysis of ovarian morphology by HE staining revealed that the number of normal follicles at all levels significantly decreased, the follicular structure was destroyed, and atretic follicles increased, while granulosa cells increased in the model rats. The study also measured important indicators of ovarian functional reserve [28], such as AMH, E_2, and FSH levels, and found that DOR rats had reduced AMH and E_2 levels and increased FSH levels. The study successfully established a DOR model in rats and found that after 10 days of treatment with either BHF or DHEA, the rats showed an increase in body weight and number of follicles at different stages, as well as a decrease in atretic follicles. Both treatments also led to an increase in AMH and E_2 levels, and a decrease in FSH levels. These findings suggest that BHF and DHEA can effectively restore ovarian function and hormonal balance in rats with DOR. Specifically, BHF restored follicle numbers at all levels and regulated reproductive hormones in rats with DOR induced by Tripterygium glycosides, thereby improving ovarian function.

Several studies have demonstrated the close association between disorders of lipid metabolism and the development of DOR [29,30]. In this study, we investigated the potential association between BHF treatment and lipid metabolism in DOR rats using UHPLC-QTOF-MS analysis. Our results showed that DOR rats exhibited disturbances in the metabolism of various lipids, including CE, DAG, HCER, LPC, PC, PE, SM, CER, and TAG. Treatment with BHF effectively modulated levels of PC, CE, DAG, and DAG, suggesting its potential therapeutic effects on lipid metabolism in DOR. Additionally, we identified 234 active ingredients of BHF by LC-MS analysis. Network pharmacology revealed that CYP19A1, CA2, CA9, ESR1, EGFR, ALOX5, AKR1B1, MAOA, ESR2, ACHE, CYP19A1, PTPN1, MAOB, PTGS1, and ADORA1 were the key genes of BHF. Through the integration of metabolomics and network pharmacology, our findings suggest that the therapeutic effects of BHF on DOR are mediated by the metabolism of linoleic acid, with the resulting metabolite being PC.

As a key component of cell membranes, PC plays a crucial role in membrane structure, fusion, and function, as well as in cellular processes such as endocytosis [31]. PC serves as a precursor for DAG, an important signaling molecule. Additionally, it plays a critical role in promoting cell proliferation, as evidenced by a lipid metabolomics analysis by Montani DA of oocytes from pregnant and non-pregnant women treated with in-vitro fertilization [32]. The analysis revealed that PC was detected only in the pregnancy group, suggesting its association with oocyte proliferation. Furthermore, PC prevented the inhibitory effect of zearalenone on oocyte maturation [33]. CE, an esterified product of cholesterol, has been found to activate the PI3K-AKT-mTOR signaling pathway, which regulates the HPOA. This leads to improved follicular development, an increase in the number of mature follicles, and enhanced ovarian reserve function [34,35]. During follicular development, DAG is produced by esterification and is stimulated by progesterone [36]. It is then released from oocytes to further stimulate follicular development. DAG binds to protein kinase C (PKC), which activates PKC and plays a pivotal role in various functions of follicular development, including cell differentiation, angiogenesis of granulosa cells, final maturation, lutealisation, and ovulation [37,38]. This study discovered that PKC triggers the expression of cyclooxygenase-2 (COX-2) in human granulosa-like cells, which leads to oocyte maturation, dilation, and ovulation [39,40]. In the present study, we found a decreasing trend of PC, CE, and DAG levels in DOR rats, which was reversed following BHF intervention. These findings suggest that BHF may promote oocyte development by modulating PC, CE, and DAG levels.

TAG, a major component of the glycerolipid family, is synthesized in the endoplasmic reticulum through the catalysis of diacylglycerol acyltransferase [41,42]. In normal conditions, TAG accounts for 60% of the neutral lipids in oocytes and is a critical energy source for oocyte maturation in bovine oocytes [43,44]. However, pathological conditions such as DOR can lead to elevated TAG levels, resulting in apoptotic cell death, indicating a possible link between TAG levels and ovarian cell apoptosis [45]. Additionally, steroid hormones have a regulatory effect on TAG levels, with post-menopausal women having higher TAG levels than pre-menopausal women. Our findings suggest that E_2 treatment can reduce TAG levels by approximately 16.4% [46,47]. The study revealed that levels of TAG in DOR rats exhibited an upward trend, but this was reversed upon intervention with BHF. These results indicate that BHF may enhance oocyte development by decreasing TAG levels.

The study suggests that the combination of metabolomics and network pharmacology indicates the importance of linoleic acid metabolism in the treatment of DOR with BHF. Linoleic acid (LA), a polyunsaturated fatty acid, is known to affect ovarian function [48]. A negative correlation between LA levels and follicle size has been reported [49], and it has been observed that LA inhibits the development of metaphase II oocytes and cumulus cell expansion [50]. The findings of the study support the link between DOR and linolenic acid metabolism, indicating that linolenic acid metabolism is closely associated with the potential of BHF to improve ovarian function in DOR.

Although the mechanism of BHF against DOR was explained through metabolic analyses and network pharmacology, this study has certain limitations that require further investigation. To address these limitations, additional pharmacological experiments are necessary for the accurate validation of the mechanisms of BHF predicted by the network pharmacology analysis. It is also important to construct metabolite-protein interactions and verify the expression of valuable proteins, as the identified differential metabolites reflect the end of biological information flow and directly reflect the status of related upstream proteins. These actions will enable a more comprehensive understanding of the underlying mechanisms involved in the potential therapeutic effects of BHF against DOR.

5. Conclusion

The study found that BHF improved ovarian function in rats with DOR induced by Tripterygium glycosides. DOR is associated with disrupted metabolism, where PC, CE, DAG, and TAG are identified as key metabolites. Our research suggests that BHF can potentially restore normal physiological functions of the ovary in DOR rats by upregulating PC, CE, and DAG, and downregulating TAG. The study also found that the key pathway to treating DOR with BHF is through linoleic acid metabolism. These metabolites and pathway are believed to play a crucial role in improving ovarian function in DOR rats treated with BHF.

Author contribution statement

Pengfei Zeng: Conceived and designed the experiments; Performed the experiments; Analyzed and interpreted the data; Wrote the paper.

Hang Zhou, Pei Guo: Performed the experiments; Analyzed and interpreted the data.

Nana Han, Xuan Zhang, Zhixing Yin, Wanting Xia: Performed the experiments; Contributed reagents, materials, analysis tools or data.

Jinzhu Huang, Qian Zeng: Conceived and designed the experiments; Analyzed and interpreted the data.

Data availability statement

Data included in article/supp. material/referenced in article.

Availability of data and materials

The data used to support the findings of this study are available from the corresponding author upon request.

Ethics approval and consent to participate

All procedures were performed in accordance with the guidelines of the Hospital of Chengdu University of Traditional Chinese Medicine ethics committee.

Funding

This work was supported by the National Natural Science Foundation of China, China (no. 82004033) and the Sichuan Province Science and Technology Support Program, China (no. 2019YFS0179).

Declaration of competing interest

The authors declare that they have no known competing financial interests or personal relationships that could have appeared to influence the work reported in this paper.

Acknowledgements

Not applicable.

Appendix A. Supplementary data

Supplementary data to this article can be found online at https://doi.org/10.1016/j.heliyon.2023.e20104.

Abbreviations

AMH	Anti-Müllerian hormone
ART	Assisted reproductive techniques
BHF	Bushen Huoxue Formula
CER	Ceramides

CE	Cholesterol esters
DOR	Diminished ovarian reserve
DHEA	Dehydroepiandrosterone
DAG	Diacylglycerols
E_2	Estradiol
ELISA	Enzyme-linked immunosorbent assay
FSH	Follicle-stimulating hormone
FFA	Free fatty acids
HE	Hematoxylin-eosin staining
HCER	Hexosylceramides
HRT	Hormone replacement therapy
HPOA	Hypothalamic-pituitary-ovarian axis
IS	Internal standard
LA	Linoleic acid
LC-MS	Liquid Chromatography-Mass Spectrometry
LPC	Lysophosphatidylcholines
LPE	Lysophosphatidylethanolamines
OPLS-DA	Orthogonal projections to latent structures-discriminant analysis
PC	phosphatidylcholines
PE	Phosphatidylethanolamines
PBS	Phosphate-buffered saline
PCA	Principal component analysis
QC	Quality control
SM	Sphingomyelins
SD	Sprague-Dawley
SPF	Specific pathogen free
TAG	Triacylglycerols
TCM	Traditional Chinese Medicine
UHPLC-QTOF-MS	Ultra High-Performance Liquid Tandem Chromatography Quadrupole Time of Flight Mass Spectrometry

References

[1] Practice Committee of the American Society for Reproductive Medicine, Electronic address: asrm@asrm.org; Practice Committee of the American Society for Reproductive Medicine. Testing and interpreting measures of ovarian reserve: a committee opinion, Fertil. Steril. 114 (6) (2020) 1151–1157, https://doi.org/10.1016/j.fertnstert.2020.09.134.

[2] J.S. Younis, R. Iskander, B.C.J.M. Fauser, et al., Does an association exist between menstrual cycle length within the normal range and ovarian reserve biomarkers during the reproductive years? A systematic review and meta-analysis, Hum. Reprod. Update 26 (6) (2020) 904–928, https://doi.org/10.1093/humupd/dmaa013.

[3] Z. Lv, Z. Lv, L. Song, et al., Role of lncRNAs in the pathogenic mechanism of human decreased ovarian reserve, Front. Genet. 14 (2023), 1056061, https://doi.org/10.3389/fgene.2023.1056061. Published 2023 Feb 8.

[4] H.X. Li, L. Shi, S.J. Liang, et al., Moxibustion alleviates decreased ovarian reserve in rats by restoring the PI3K/AKT signaling pathway, J Integr Med 20 (2) (2022) 163–172, https://doi.org/10.1016/j.joim.2022.01.007.

[5] Committee opinion no, 618: ovarian reserve testing, Obstet. Gynecol. 125 (1) (2015) 268–273, https://doi.org/10.1097/01.AOG.0000459864.68372.ec.

[6] Q.L. Zhang, Y.L. Lei, Y. Deng, et al., Treatment progress in diminished ovarian reserve: western and Chinese medicine, Chin. J. Integr. Med. 29 (4) (2023) 361–367, https://doi.org/10.1007/s11655-021-3353-2.

[7] S. Agarwal, F.A. Alzahrani, A. Ahmed, Hormone replacement therapy: would it be possible to replicate a functional ovary? Int. J. Mol. Sci. 19 (10) (2018) 3160, https://doi.org/10.3390/ijms19103160.

[8] K. Yakin, B. Urman, DHEA as a miracle drug in the treatment of poor responders; hype or hope? Hum. Reprod. 26 (8) (2011) 1941–1944, https://doi.org/10.1093/humrep/der150.

[9] Y. Xu, V. Nisenblat, C. Lu, et al., Pretreatment with coenzyme Q10 improves ovarian response and embryo quality in low-prognosis young women with decreased ovarian reserve: a randomized controlled trial, Reprod. Biol. Endocrinol. 16 (1) (2018) 29, https://doi.org/10.1186/s12958-018-0343-0.

[10] L. Han, H. Tian, X. Guo, et al., Regulation of ovarian function by growth hormone: potential intervention of ovarian aging, Front. Endocrinol. 13 (2023), 1072313, https://doi.org/10.3389/fendo.2022.1072313.

[11] M.A. Youssef, M. van Wely, M. Mochtar, et al., Low dosing of gonadotropins in in vitro fertilization cycles for women with poor ovarian reserve: systematic review and meta-analysis, Fertil. Steril. 109 (2) (2018) 289–301, https://doi.org/10.1016/j.fertnstert.2017.10.033.

[12] W. Xu, M. Tang, J. Wang, et al., Clinical effects of Shou-Wu Jiang-Qi Decoction combined acupuncture on the treatment of Polycystic Ovarian Syndrome with kidney deficiency, phlegm and blood stasisness: study protocol clinical trial (SPIRIT Compliant), Medicine (Baltim.) 99 (12) (2020), e19045, https://doi.org/10.1097/MD.0000000000019045.

[13] J. Song, T. Ma, Y. Liang, et al., Efficacy and safety of Dingkun pill for female infertility patients with low prognosis undergoing in vitro fertilization-embryo transfer: study protocol for a multicenter, double-blind, randomized, placebo-controlled trial, Trials 21 (1) (2020) 550, https://doi.org/10.1186/s13063-020-04502-z.

[14] W. Duan, Y. Cheng, Sequential therapy for kidney-tonifying via traditional Chinese medicine effectively improves the reproductive potential and quality of life of women with decreased ovarian reserve: a randomized controlled study, Am J Transl Res 13 (4) (2021) 3165–3173.

[15] M. Jiang, W. Wang, J. Zhang, et al., Protective effects and possible mechanisms of actions of bushen cuyun recipe on diminished ovarian reserve induced by cyclophosphamide in rats, Front. Pharmacol. 11 (2020) 546, https://doi.org/10.3389/fphar.2020.00546.

[16] L. Gao, Y. Zhang, H. Xu, et al., Therapeutic effects of modified gengnianchun formula on stress-induced diminished ovarian reserve based on experimental approaches and network pharmacology [published correction appears in drug des devel ther. 2021 jan 27;15:349], Drug Des Devel Ther 14 (2020) 4975–4992, https://doi.org/10.2147/DDDT.S279553.
[17] F. Zhao, W. Wang, Gengnianchun recipe protects ovarian reserve of rats treated by 4-vinylcyclohexene diepoxide via the AKT pathway, Int J Endocrinol 2020 (2020), 9725898, https://doi.org/10.1155/2020/9725898.
[18] S. Abou el Ela Ael, A.A. Allam, E.H. Ibrahim, Pharmacokinetics and anti-hypertensive effect of metoprolol tartrate rectal delivery system, Drug Deliv. 23 (1) (2016) 69–78, https://doi.org/10.3109/10717544.2014.904021.
[19] S. Hua, Physiological and pharmaceutical considerations for rectal drug formulations, Front. Pharmacol. 10 (2019) 1196, https://doi.org/10.3389/fphar.2019.01196.
[20] H. Zhou, P. Guo, P. Zeng, et al., Effect of zhuyun I recipe capsule enema on the immune microenvironment of the endometrium during implantation window in rats, Emerg Med Int 2022 (2022), 4746121, https://doi.org/10.1155/2022/4746121.
[21] P. Wang, Q. Wang, B. Yang, et al., The progress of metabolomics study in traditional Chinese medicine research, Am. J. Chin. Med. 43 (7) (2015) 1281–1310, https://doi.org/10.1142/S0192415X15500731.
[22] C. Nogales, Z.M. Mamdouh, M. List, , et al.A.I. Casas, H.H.H.W. Schmidt, Network pharmacology: curing causal mechanisms instead of treating symptoms, Trends Pharmacol. Sci. 43 (2) (2022) 136–150, https://doi.org/10.1016/j.tips.2021.11.004.
[23] Z. Pang, J. Chong, G. Zhou, et al., MetaboAnalyst 5.0: narrowing the gap between raw spectra and functional insights, Nucleic Acids Res. 49 (W1) (2021) W388–W396, https://doi.org/10.1093/nar/gkab382.
[24] W. Zhang, Y. Chen, H. Jiang, et al., Integrated strategy for accurately screening biomarkers based on metabolomics coupled with network pharmacology, Talanta 211 (2020), 120710, https://doi.org/10.1016/j.talanta.2020.120710.
[25] Y. Zhou, B. Zhou, L. Pache, et al., Metascape provides a biologist-oriented resource for the analysis of systems-level datasets, Nat. Commun. 10 (1) (2019) 1523, https://doi.org/10.1038/s41467-019-09234-6.
[26] P. Deng, H. Liang, S. Wang, et al., Combined metabolomics and network pharmacology to elucidate the mechanisms of Dracorhodin Perchlorate in treating diabetic foot ulcer rats, Front. Pharmacol. 13 (2022), 1038656, https://doi.org/10.3389/fphar.2022.1038656.
[27] S. Liang, Y. Chen, Q. Wang, et al., Prevalence and associated factors of infertility among 20-49 year old women in Henan Province, China, Reprod. Health 18 (1) (2021) 254, https://doi.org/10.1186/s12978-021-01298-2.
[28] X. Jiao, T. Meng, Y. Zhai, et al., Ovarian reserve markers in premature ovarian insufficiency: within different clinical stages and different etiologies, Front. Endocrinol. 12 (2021), 601752, https://doi.org/10.3389/fendo.2021.601752.
[29] E. Warzych, P. Lipinska, Energy metabolism of follicular environment during oocyte growth and maturation, J. Reprod. Dev. 66 (1) (2020) 1–7, https://doi.org/10.1262/jrd.2019-102.
[30] L. Sanchez-Lazo, D. Brisard, S. Elis, et al., Fatty acid synthesis and oxidation in cumulus cells support oocyte maturation in bovine, Mol. Endocrinol. 28 (9) (2014) 1502–1521, https://doi.org/10.1210/me.2014-1049.
[31] Z. Li, D.E. Vance, Phosphatidylcholine and choline homeostasis, J. Lipid Res. 49 (6) (2008) 1187–1194, https://doi.org/10.1194/jlr.R700019-JLR200.
[32] D.A. Montani, F.B. Cordeiro, T. Regiani, et al., The follicular microenviroment as a predictor of pregnancy: MALDI-TOF MS lipid profile in cumulus cells, J. Assist. Reprod. Genet. 29 (11) (2012) 1289–1297.
[33] F.N. Lai, X.L. Liu, N. Li, et al., Phosphatidylcholine could protect the defect of zearalenone exposure on follicular development and oocyte maturation, Aging (Albany NY) 10 (11) (2018) 3486–3506.
[34] T.Y. Chang, B.L. Li, C.C. Chang, et al., Acyl-coenzyme A:cholesterol acyltransferases, Am. J. Physiol. Endocrinol. Metab. 297 (1) (2009) E1–E9, https://doi.org/10.1152/ajpendo.90926.2008.
[35] J. Li, D. Gu, S.S. Lee, et al., Abrogating cholesterol esterification suppresses growth and metastasis of pancreatic cancer, Oncogene 35 (50) (2016) 6378–6388, https://doi.org/10.1038/onc.2016.168.
[36] X. Wen, Y. Kuang, L. Zhou, et al., Lipidomic components alterations of human follicular fluid reveal the relevance of improving clinical outcomes in women using progestin-primed ovarian stimulation compared to short-term protocol, Med Sci Monit 24 (2018) 3357–3365, https://doi.org/10.12659/MSM.906602.
[37] M. Cooke, A. Magimaidas, V. Casado-Medrano, et al., Protein kinase C in cancer: the top five unanswered questions, Mol. Carcinog. 56 (6) (2017) 1531–1542, https://doi.org/10.1002/mc.22617.
[38] P.G. Tremblay, M.A. Sirard, Transcriptomic analysis of gene cascades involved in protein kinase A and C signaling in the KGN line of human ovarian granulosa tumor cells, Biol. Reprod. 96 (4) (2017) 855–865, https://doi.org/10.1093/biolre/iox024.
[39] Y.Y. Lin, D. Sun, Y.L. Wu, Novel regulation of PKC-induced inflammation by Akt and protein phosphatase 2A in ovarian granulosa cells, Chin. J. Physiol. 63 (4) (2020) 179–186, https://doi.org/10.4103/CJP.CJP_44_20.
[40] H.L. Ou, D. Sun, Y.C. Peng, et al., Novel effects of the cyclooxygenase-2-selective inhibitor NS-398 on IL-1β-induced cyclooxygenase-2 and IL-8 expression in human ovarian granulosa cells, Innate Immun. 22 (6) (2016) 452–465, https://doi.org/10.1177/1753425916654011.
[41] C.L. Yen, S.J. Stone, S. Koliwad, at al, Thematic review series: glycerolipids. DGAT enzymes and triacylglycerol biosynthesis, J. Lipid Res. 49 (11) (2008) 2283–2301, https://doi.org/10.1194/jlr.R800018-JLR200.
[42] A.R. Thiam, M. Beller, The why, when and how of lipid droplet diversity, J. Cell Sci. 130 (2) (2017) 315–324, https://doi.org/10.1242/jcs.192021.
[43] R. Santos, R. Rosas-Oliveira, F.B. Saraiva, et al., Lipid accumulation and utilization by oocytes and eggs of Rhodnius prolixus, Arch. Insect Biochem. Physiol. 77 (1) (2011) 1–16, https://doi.org/10.1002/arch.20414.
[44] E.M. Ferguson, H.J. Leese, A potential role for triglyceride as an energy source during bovine oocyte maturation and early embryo development, Mol. Reprod. Dev. 73 (9) (2006) 1195–1201, https://doi.org/10.1002/mrd.20494.
[45] N.M. Al-Saffar, J.C. Titley, D. Robertson, et al., Apoptosis is associated with triacylglycerol accumulation in Jurkat T-cells, Br. J. Cancer 86 (6) (2002) 963–970, https://doi.org/10.1038/sj.bjc.6600188.
[46] S. Santosa, M.D. Jensen, Adipocyte fatty acid storage factors enhance subcutaneous fat storage in postmenopausal women, Diabetes 62 (3) (2013) 775–782, https://doi.org/10.2337/db12-0912.
[47] F. Luo, W.Y. Huang, Y. Guo, et al., 17β-estradiol lowers triglycerides in adipocytes via estrogen receptor α and it may be attenuated by inflammation, Lipids Health Dis. 16 (1) (2017) 182, https://doi.org/10.1186/s12944-017-0575-6.
[48] A. Catalá, Five decades with polyunsaturated Fatty acids: chemical synthesis, enzymatic formation, lipid peroxidation and its biological effects, J Lipids 2013 (2013), 710290, https://doi.org/10.1155/2013/710290.
[49] S.T. Homa, C.A. Brown, Changes in linoleic acid during follicular development and inhibition of spontaneous breakdown of germinal vesicles in cumulus-free bovine oocytes, J. Reprod. Fertil. 94 (1) (1992) 153–160, https://doi.org/10.1530/jrf.0.0940153.
[50] W.F. Marei, D.C. Wathes, A.A. Fouladi-Nashta, Impact of linoleic acid on bovine oocyte maturation and embryo development, Reproduction 139 (6) (2010) 979–988, https://doi.org/10.1530/REP-09-0503.